

Discovery and Analysis of Time Delay Sources in the USGS Personal Computer Data Collection Platform (PCDCP) System



Scientific Investigations Report 2014–5045

COVER. Locations of geomagnetic observatories operated by the U.S. Geological Survey and partners of the U.S. Geological Survey Geomagnetism Program.

Discovery and Analysis of Time Delay Sources in the USGS Personal Computer Data Collection Platform (PCDCP) System

By Timothy C. White, Edward A. Sauter, and Duff C. Stewart

Scientific Investigations Report 2014–5045

U.S. Department of the Interior
U.S. Geological Survey

U.S. Department of the Interior
SALLY JEWELL, Secretary

U.S. Geological Survey
Suzette M. Kimball, Acting Director

U.S. Geological Survey, Reston, Virginia: 2014

For more information on the USGS—the Federal source for science about the Earth, its natural and living resources, natural hazards, and the environment, visit <http://www.usgs.gov> or call 1–888–ASK–USGS.

For an overview of USGS information products, including maps, imagery, and publications, visit <http://www.usgs.gov/pubprod>

To order this and other USGS information products, visit <http://store.usgs.gov>

Any use of trade, firm, or product names is for descriptive purposes only and does not imply endorsement by the U.S. Government.

Although this information product, for the most part, is in the public domain, it also may contain copyrighted materials as noted in the text. Permission to reproduce copyrighted items must be secured from the copyright owner.

Suggested citation:

White, T.C., Sauter, E.A., and Stewart, D.C., 2014, Discovery and analysis of time delay sources in the USGS personal computer data collection platform (PCDCP) system: U.S. Geological Survey Scientific Investigations Report 2014–5045, 24 p., <http://dx.doi.org/10.3133/sir20145045>.

ISSN 2328-0328 (online)

Contents

Abstract.....	1
Introduction.....	1
Elements of the USGSGP Geomagnetic Data Collection System.....	1
Narod Magnetometer	2
Thunderbolt GPS Disciplined Clock—Primary Timing Source.....	2
Lawson Model 802 Electronic Data-Collection Module.....	4
Master Data-Collection Board	4
Temperature Information.....	4
System Power Information.....	5
Slave Data-Collection Board	6
Triggering/Time Stamping.....	6
Gem Systems GSM-19 Overhauser Magnetometer.....	6
Data Transport and Digital Filtering.....	7
Method for Testing Delay	8
Individual Component Tests	8
Sine-Wave Test	8
Introduction	8
Test Setup.....	8
Pre-Test Measurements	8
Test Results.....	8
Square-Wave Test	8
Introduction	8
Test Setup.....	8
Pre-Test Measurements	10
Test Results.....	10
Lawson Model 802 Square-Wave Test.....	10
Introduction	10
Test Setup.....	11
Pre-Test Measurements	11
Test Results.....	11
Overall System Test.....	12
Jean Rasson Test.....	12
Test Setup.....	12
Pre-Test Measurements	12
Test Results.....	12
Berkeley Nucleonics Corp. BNC 565 Test.....	12
Introduction	12
Pre-Test Measurements	12
Test Results.....	12
Analysis and Summary of Results of Delay Testing	12
Narod Magnetometer	14
Lawson Model 802 Data-Collection Electronic Module.....	14

Overall System Tests	14
Summary.....	15
References Cited.....	15
Glossary.....	17
Appendix A. Design of Personal Computer Data-Collection Platform Gaussian Filters.....	19
Appendix A–1. Design of the Personal Computer Data-Collection Platform	
One-Minute Gaussian Filter.....	19
Step Two: Calculate the Value of σ , Sigma	19
Step Three: Calculate and Normalize Filter Coefficients	19
Appendix A–2. Design of the Personal Computer Data-Collection Platform	
One-Second Gaussian Filter.....	21

Figures

1. Data-flow diagram for the Personal Computer Data Collection Platform (PCDCP) showing major electronic components	2
2. Gain characteristics for the Butterworth filter in the Narod magnetometer	3
3. Phase characteristics for the Butterworth filter within the Narod magnetometer, where time offset is represented in seconds and negative time represents a lag	3
4. Pulse-per-second (PPS) signal from the Thunderbolt GPS Disciplined Clock (T-Bolt) timing source as measured by an oscilloscope.....	4
5. Data flow within the Lawson Model 802 data-collection electronics module	5
6. Examples of possible timing states for the Model 802 data-collection electronic module	6
7. Gem Systems GSM-19 Overhauser magnetometer sampling methodology	7
8. Sine-wave test setup for characterizing delay in the Narod magnetometer.....	9
9. Signal delay in the Narod magnetometer as measured by oscilloscope across a 1-ohm test resistor on the trailing edge of the coil circuit.....	9
10. Square-wave test setup for characterization of delay in the Narod magnetometer using a Berkeley Nucleonics Corp. BNC 565 pulse/delay generator.....	10
11. Square-wave test setup for characterization of delay in the Lawson Model 802 data-collection module using a Berkeley Nucleonics Corp. BNC 565 pulse/delay generator.....	11
12. Customized Black Box pulse-per-second (PPS) signal (red) in relation to the T-Bolt clock PPS signal (blue), as shown on oscilloscope screen in the Rasson overall system test.....	13
13. Example of Gaussian filter weighting function applied over four seconds of 100-Hz data	17
A–1. Normalized coefficients of the one-minute Gaussian filter.....	20
A–2. Normalized coefficients of the one-second Gaussian filter.....	21

Tables

1.	Expected average delay and delay range for each magnetic component in the Model 802 electronic module	7
2.	Specifications of the Narod magnetometer customized test coil	8
3.	Sine-wave results at test frequencies for the H (north/south) axis of the Narod magnetometer sensor	10
4.	Step response test results for square-wave testing of the Narod magnetometer	10
5.	Jean Rasson test results for overall system delay	13
6.	Delay-test results using the Berkeley Nucleonics Corp. BNC 565 pulse generator	13
7.	Summary of all results from delay tests.....	14
A-1.	Filter coefficients for the Personal Computer Data-Collection Platform one-minute Gaussian filter. Precision is set to six significant figures, consistent with similar USGSGP calculations.....	20
A-2.	Filter coefficients for the Personal Computer Data-Collection Platform one-second Gaussian filter	22

Conversion Factors

SI to Inch/Pound

Multiply	By	To obtain
	Length	
centimeter (cm)	0.3937	inch (in.)
meter (m)	3.281	foot (ft)

Temperature in degrees Celsius (°C) may be converted to degrees Fahrenheit (°F) as follows:

$$^{\circ}\text{F} = (1.8 \times ^{\circ}\text{C}) + 32$$

Abbreviated Units

cm	centimeter
dB	decibel
°C	temperature, degrees Celsius
Hz	Hertz
ms	millisecond
nT	nanoTesla, magnetic field strength, one-billionth of a Tesla
s	second
μs	microsecond
V	volts

Abbreviations and Acronyms

ADC	analog-to-digital converter
D,	axis east/west magnetic field component
H,	axis north/south magnetic field component
PCDCP	Personal Computer Data Collection Platform
PPS	pulse per second
UTC	Coordinated Universal Time
VAC	voltage, alternating current
VDC	voltage, direct current
Z,	axis vertical magnetic field component

Discovery and Analysis of Time Delay Sources in the USGS Personal Computer Data Collection Platform (PCDCP) System

By Timothy C. White, Edward A. Sauter and Duff C. Stewart

Abstract

Intermagnet is an international oversight group which exists to establish a global network for geomagnetic observatories. This group establishes data standards and standard operating procedures for members and prospective members. Intermagnet has proposed a new One-Second Data Standard, for that emerging geomagnetic product. The standard specifies that all data collected must have a time stamp accuracy of ± 10 milliseconds of the top-of-the-second Coordinated Universal Time. Therefore, the U.S. Geological Survey Geomagnetism Program has designed and executed several tests on its current data collection system, the Personal Computer Data Collection Platform. Tests are designed to measure the time shifts introduced by individual components within the data collection system, as well as to measure the time shift introduced by the entire Personal Computer Data Collection Platform. Additional testing designed for Intermagnet will be used to validate further such measurements. Current results of the measurements showed a 5.0–19.9 millisecond lag for the vertical channel (Z) of the Personal Computer Data Collection Platform and a 13.0–25.8 millisecond lag for horizontal channels (H and D) of the collection system. These measurements represent a dynamically changing delay introduced within the U.S. Geological Survey Personal Computer Data Collection Platform.

Introduction

The U.S. Geological Survey Geomagnetism Program (USGSGP) seeks to measure time shifts introduced by the data collection system it currently uses at 14 magnetic observatories located across the United States and its territories. Measurements made using the USGSGP Personal Computer Data Collection Platform (PCDCP) are required to establish compliance for data quality with the proposed Intermagnet One-Second Data Standards (C.W. Turbitt, British Geological Survey National Environment Research Council, oral

commun., June 2012). According to those international standards, all collected one-second data must have a timing accuracy of ± 10 milliseconds (ms) of Coordinated Universal Time (UTC). All one-second data points must have any introduced time shifts smaller than ± 10 ms of the top-of-the-second UTC.

Measurements are designed and performed to identify not only the average time shift introduced by the composite data collection platform but also that time shift introduced by individual components within the data collection system. Methods used to measure the time shifts provide insight to the internal functionality of the system. The results of such measurements potentially improve data quality and assist in future development of these data collection systems.

Testing also addressed the viability of other measurement methods. Those methods have been proposed for use within the international geomagnetic observatory community. Inaccuracies and inconsistencies in such methods would have tremendous impacts on the geomagnetic community at large.

Elements of the USGSGP Geomagnetic Data Collection System

The U.S. Geological Survey Geomagnetism Program deploys a custom-designed and manufactured data-collection system called the Personal Computer Data Collection Platform (PCDCP). Two sensors provide a real-time data feed of the Earth's magnetic activity, and another sensor records vector data for each of three axes. An additional sensor measures the total magnitude of the magnetic field vector. A global positioning system discipline clock provides an accurate time stamp for the data. A high-resolution analog-to-digital converter captures measured vector data. Other environmental characteristics also are monitored by the PCDCP system. Figure 1 illustrates data flow within PCDCP from the sensors to the acquisition computer. Each of these components will be discussed to understand better the contribution of each to the total time shift.

2 Discovery and Analysis of Time Delay Sources in the Data Collection Platform System

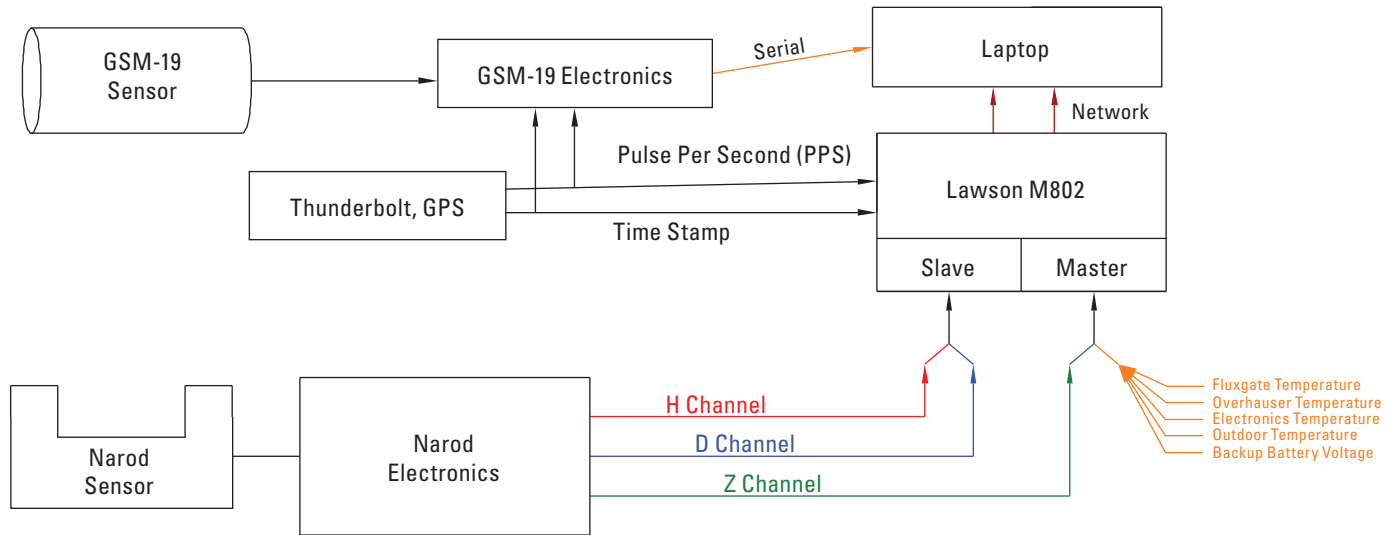


Figure 1. Data-flow diagram for the Personal Computer Data Collection Platform (PCDCP) showing major electronic components. [Z, vertical magnetic field component; H, north/south field component; D, east/west component; GPS, global positioning system]

Narod Magnetometer

The Narod ring-core magnetometer, or Narod, is a tri-axial magnetometer used by PCDCP. This sensor measures the magnetic field along three mutually orthogonal axes. The Narod is an auto-biasing magnetometer designed to optimize the analog input range of an analog-to-digital converter (ADC) by introducing bias fields into each individual axis of the sensor. The principle of superposition was applied such that the bias field negates most of the field incident on the sensor. Output of any remaining field measurement by the sensor is an analog voltage signal.

As an example, a 10,242-nanotesla (nT) natural field incident on the H-axis of the sensor would produce the following functionality of the Narod (fig. 2). The Narod electronics would introduce 10,000 nT of bias field within the H-axis of the sensor.

Bias increments were 500 nT for all three axes, therefore, in this example, the electronics would introduce 20 bias increments opposing the natural field. By superposition, the bias field would cancel most of the natural field. The remaining 242 nT (after cancellation of the 20 increments of 500 nT each) then would be measured by the sensor. As noted above, that measurement is put out as an analog voltage. A scale value is applied to the voltage to convert back into nanoteslas (nT). The Narod has nominal scale values of 100 nT/volt for all three axes. Using the example, the analog output of the Narod magnetometer would be 2.42 volts (V). The Narod would have a digital output of 20 for the H-axis, corresponding to the number of introduced bias increments.

The analog signal is filtered within the Narod electronics before analog output by a three-pole Butterworth low-pass filter, referred to as a Butterworth (Narod, 2000). The corner

frequency used by the USGSGP typically is 50 hertz (Hz). That corner frequency attenuates 60-Hz noise introduced by common alternating-current (VAC) power and prevents anti-aliasing the 100-Hz samples collected by the ADC. Presently, all USGSGP observatories are located within the United States and its territories, where 60-Hz VAC power is the established standard.

The Butterworth filter has a very linear or “flat” gain characteristic up to the corner frequency, as well as other useful characteristics. Figure 2 shows the Bode plot of the gain characteristic for the three-pole Butterworth low-pass filter. Since no ripple appears in the gain curve (fig. 2), the Butterworth is an ideal selection for instrumentation applications. The Butterworth also has a desirable phase response (fig. 3). Phase response is a representation of the time lag introduced to a signal at given frequency passed through the filter. The Butterworth introduces a near-constant time lag for all frequencies less than the corner frequency. Analysis of the phase response for the Butterworth indicates an expected time lag of about 6 ms. Additionally, there is an expected time lag of 5 ms from the sensor as well (B.B. Narod, University of British Columbia, oral commun., October 2012). By superposition, the total expected time lag is 11 ms.

Thunderbolt GPS Disciplined Clock—Primary Timing Source

The primary timing source used by PCDCP is the Thunderbolt GPS Disciplined Clock (referred to as the T-Bolt) manufactured by Trimble Navigation, Ltd. The T-Bolt produces highly accurate and stable timing information. The clock is heated internally to maintain a constant-temperature

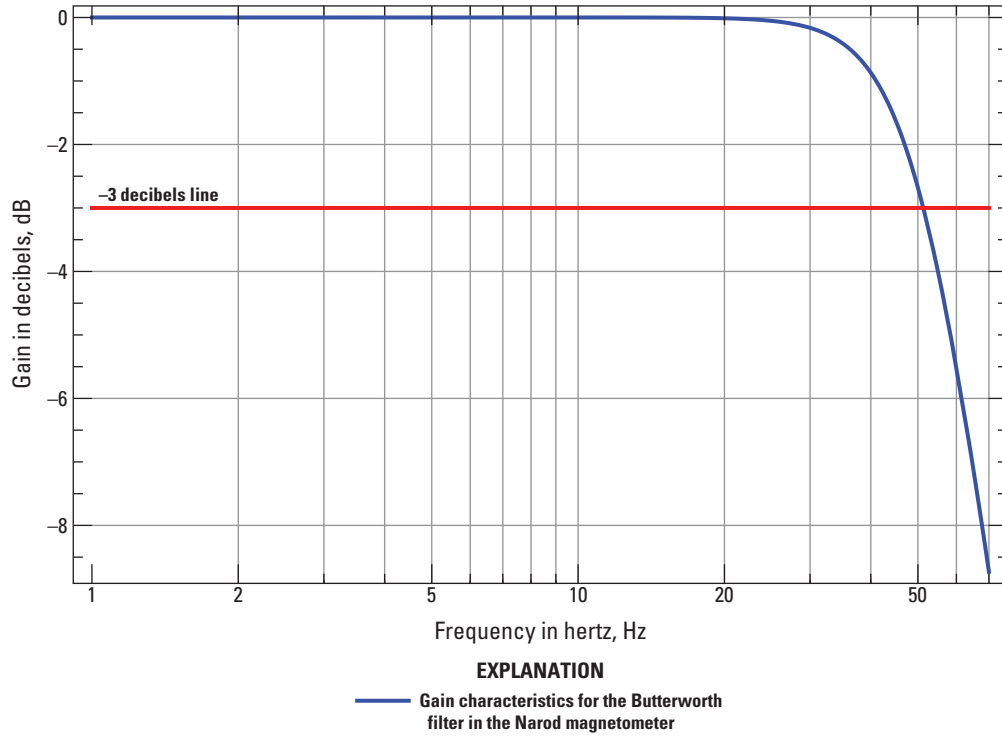


Figure 2. Gain characteristics for the Butterworth filter in the Narod magnetometer.

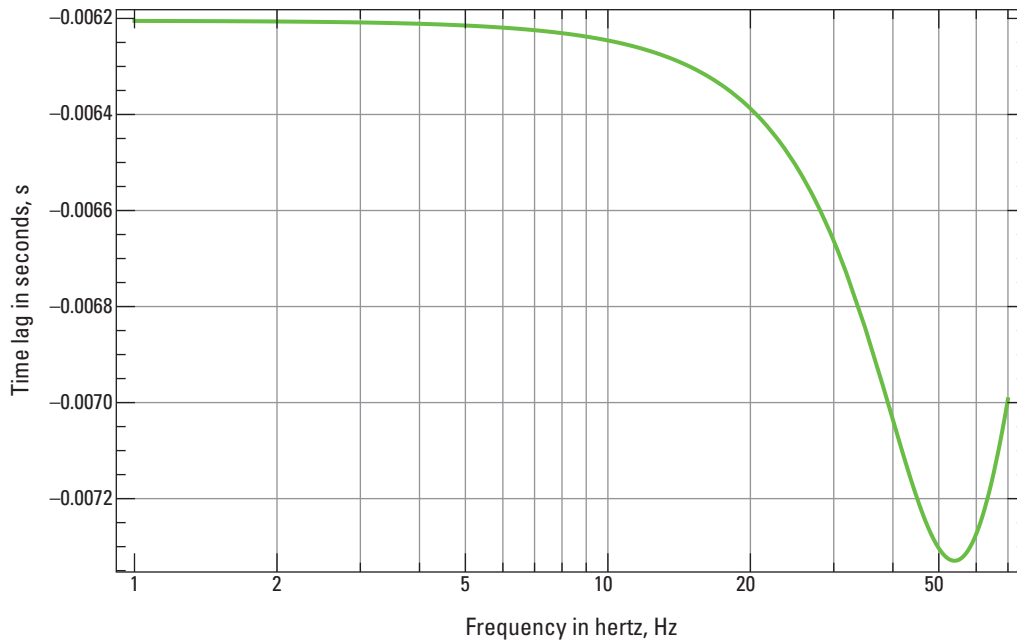


Figure 3. Phase characteristics for the Butterworth filter within the Narod magnetometer, where time offset is represented in seconds and negative time represents a lag.

4 Discovery and Analysis of Time Delay Sources in the Data Collection Platform System

operating environment for the timing crystal. The crystal is synchronized to the global positioning system (GPS), and the T-Bolt is configured to a Coordinated Universal Time (UTC) output. A correction between GPS and UTC, broadcast by the GPS system is required. A pulse-per-second signal (PPS) is put out by the T-Bolt with a stated accuracy of ± 20 ns to the top of the second of UTC (Trimble, 2011), and the T-Bolt signal is measured with an oscilloscope. The oscilloscope (fig. 4) measures the square PPS pulse which had amplitude of about 4.5 V and a width of 10.0 microseconds (μ s).

The T-Bolt also releases digital time-stamp information through a serial connection. The PCDCP uses both the PPS signal and digital time-stamp data. Application of these signals will be explained in the section describing the Lawson 802 module.

Lawson Model 802 Electronic Data-Collection Module

The Lawson Labs, Inc., Model 802 (802) electronics module provides the central data node within PCDCP. The 802 has several internal components, including ADCs, a digital input, and Ethernet controllers (see fig. 5). The 802 has two data-collection boards, referred to as the slave and the master. Each board houses a 24-bit ADC.

Master Data-Collection Board

The analog signal for the vertical component of the magnetic field passes into the master data-collection board. The vertical component is multiplexed (see Glossary) with the “housekeeping” signals for PCDCP. Five housekeeping signals are all multiplexed together and include four temperature measurements and a system battery-voltage reading.

Temperature Information

Temperature fluctuations have an undesirable effect on PCDCPs. The Narod sensor and Narod magnetometer electronics have temperature coefficients that could delineate the data. The stated temperature coefficients were 0.1 nT/ $^{\circ}$ C (Narod, 2000) for the sensor and 0.2 nT/ $^{\circ}$ C for the sensor electronics, although higher effects have been observed. Four temperatures are measured and monitored using temperature transducers. In general, the USGSGP has established a temperature stability goal of ± 3 $^{\circ}$ C for all instrumentation areas. Temperature transducers monitor temperature variations to identify thermal effects. One temperature transducer usually is placed about 30 cm above the Narod sensor. A second temperature transducer is placed within the housing of the data-collection hardware, also approximately 30 cm from the Narod electronics. A third temperature transducer is placed in close proximity to the Overhauser sensor. The Overhauser sensor temperature

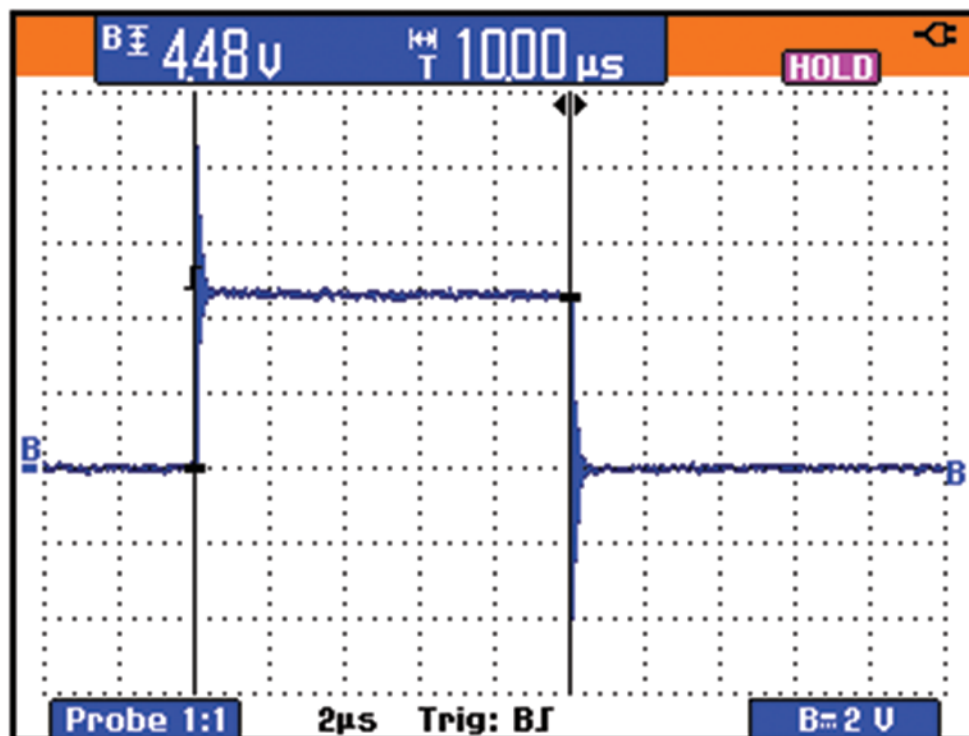


Figure 4. Pulse-per-second (PPS) signal from the Thunderbolt GPS Disciplined Clock (T-Bolt) timing source as measured by an oscilloscope.

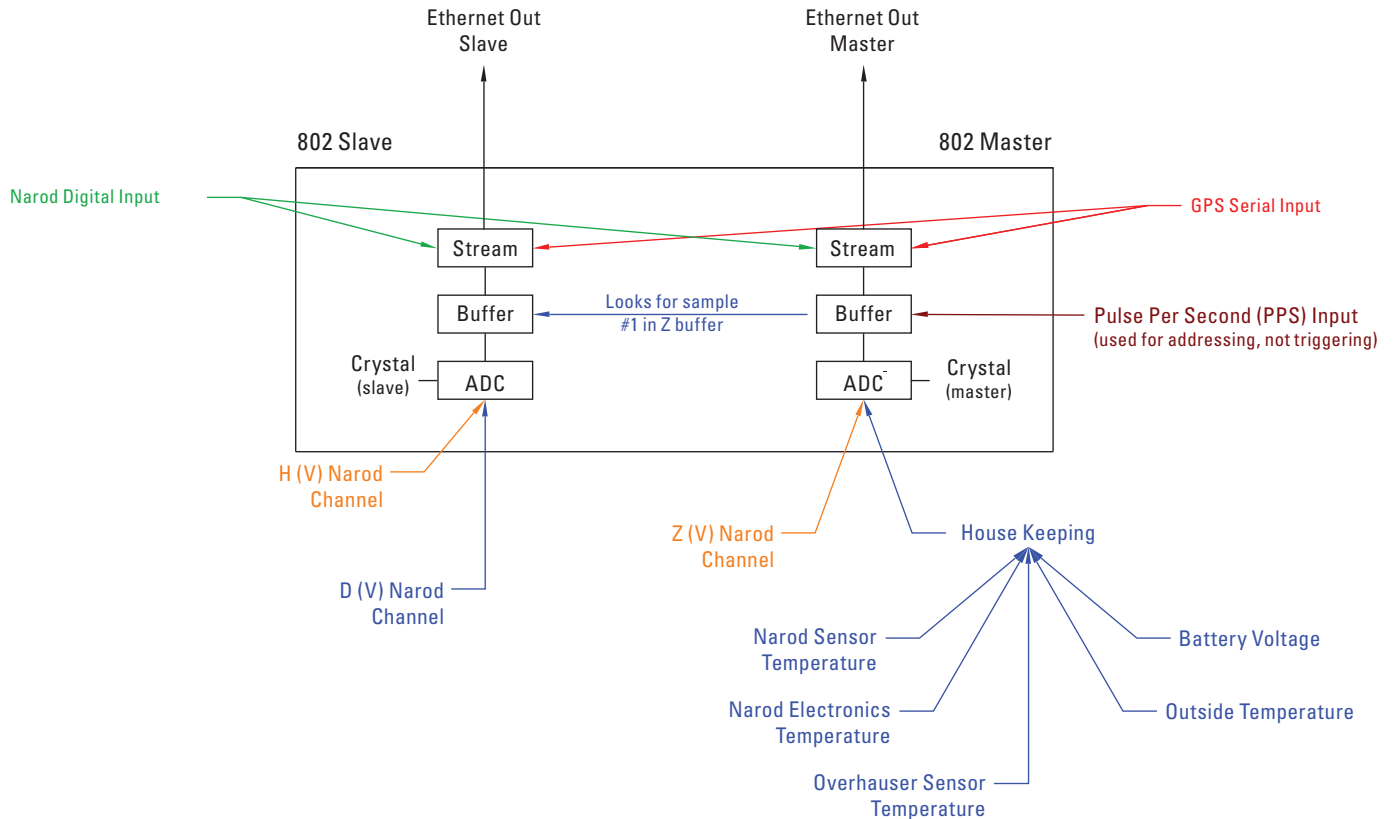


Figure 5. Data flow within the Lawson Model 802 data-collection electronics module. [ADC, analog-to-digital converter; PPS, pulse per second; GPS, global positioning system; Z, vertical magnetic field component (volts); H, north/south field component (volts); D, east/west component (volts); V, volts]

coefficient is not specified by the manufacturer (Gem Systems Advanced Magnetometers, Inc., Markham, Ontario, 2012, available at www.gemsys.ca/products/rugged-overhauser-magnetometer/, last accessed December 21, 2012), however, effects of 0.25 nT/°C have been observed by the USGSGP. Stated absolute accuracy of the Overhauser is ±0.2 nT over the full operating temperature range of the sensor. The fourth temperature transducer, placed outside the primary instrumentation building, monitors the overall effectiveness of the temperature-control system and the building insulation.

System Power Information

The USGSGP spent substantial time developing the power system for the PCDCP, which is powered using a switching direct current (VDC) power supply. The power supply has an input of 120 VAC and output of 24 VDC. The output passes to a custom power-distribution board, where VDC to VDC converters provide 12 VDC and 9 VDC to power various hardware components of PCDCP. If VAC power were lost, the PCDCP is backed up with a 24-VDC battery bank. The voltage level of this battery bank is monitored by the PCDCP.

The five housekeeping signals pass into a multiplexer. That multiplexer operates in a free running mode as the housekeeping signals are not time-critical. The multiplexed housekeeping signal passes to a second multiplexer, which switches between the housekeeping signal and the vertical (Z) magnetic field signal. The PPS from the T-bolt clock synchronizes the second multiplexer such that the Z signal always is sampled within 5 ms of the PPS arrival. The multiplexed signal then passes to the analog-to-digital converter (ADC).

The ADC samples at a rate of 1000.65 Hz, where the frequency is controlled by a free-running, internal clock. The multiplexer switches between two channels, A and B. Channel A is sampled five times by the 1000.65-Hz ADC. The first four of these 1000.65-Hz samples are ignored and the fifth passes to the data buffer. Ignoring the four 1000.65-Hz samples allows the ADC time to purge an internal digital buffer and prevent charge pumpout (see Glossary). The process of throwing out 80% of the samples establishes the 802's effective sampling rate of 200.13 Hz. The multiplexer then switches to channel B, and the ADC samples it five times. Again, the first four samples are ignored, and the fifth passes into the data buffer. After this multiplexing, the effective sampling rate becomes 100.065 Hz for each channel A and B.

Slave Data-Collection Board

The hardware within the slave electronics board basically is identical to the master. However, a few differences should be noted. Many such differences relate to the data stream once it passes into the data buffer. (Such differences will be addressed in a later section.) Only two channels of data are processed by the slave board, the north/south (H) and east/west (D) data components for the magnetic field. These channels are multiplexed. Unlike the master board where the multiplexer is synchronized such that the Z component channel is sampled within 5 ms of the pulse-per-second signal (PPS), the multiplexer on the slave is free-running, meaning that the H component or D component could be sampled closer to the PPS (fig. 6). The ADC on the slave operates in the same manner as the ADC on the master. The digitized data pass into a data buffer where timing standards are applied.

Triggering/Time Stamping

The pulse-per-second signal (PPS) from the T-Bolt clock labels the first sample of the Z channel after the PPS as the “number one” sample for that second (Lawson Labs, Inc., Malvern, Pa., oral commun., 2010). During initialization, the 802 approximately synchronizes the two-channel multiplexer on the master such that the Z channel always is sampled within 5 ms of the PPS. Note that the timing of the five-signal multiplexed housekeeping channel is not important, and therefore a lower priority is placed on the time-stamp accuracy of those data. The 802 module scans the data buffer of the Z channel for the “number-one” sample. Once Z sample number one is detected, the 802 labels the next samples taken on both

the H and D components as “number one” in their respective data buffers. Since H and D cannot be labeled until Z has been labeled, the minimum delay for H and D would be the same as that for Z. The maximum delay would then be one complete sampling period after the latest moment Z could have been labeled, yielding a maximum delay of about 14.9 ms (fig. 6). Table 1 shows the delay ranges expected to be introduced from this configuration of the 802. It is important to note that both the Master ADC and Slave ADC have sampling controlled by independent timing crystals, and therefore sampling of the “number-one” sample could drift in time relative to the PPS. The absolute difference in time between the “number-one” sample on the Z channel and the “number-one” samples for the H and D channels could also drift over time.

Gem Systems GSM-19 Overhauser Magnetometer

In addition to the vector data measured by the Narod magnetometer, the PCDCP also uses a Gem Systems GSM-19 Overhauser total field magnetometer (referred to as the GSM-19). The GSM-19 measures the magnitude of the magnetic field through a proton precession process. Unlike the Narod, the GSM-19 does not provide a continuous signal. The one-second sampling setting on the GSM-19 is used by PCDCP.

The PPS from the T-Bolt clock triggers an initialization and polarization event within the sensor. Polarization takes 35 ms (Gem Systems Advanced Magnetometers, Inc., 2009), at the end of which the sensor begins sampling the precession within the sensor (fig. 7). The oscillating signal slowly decays

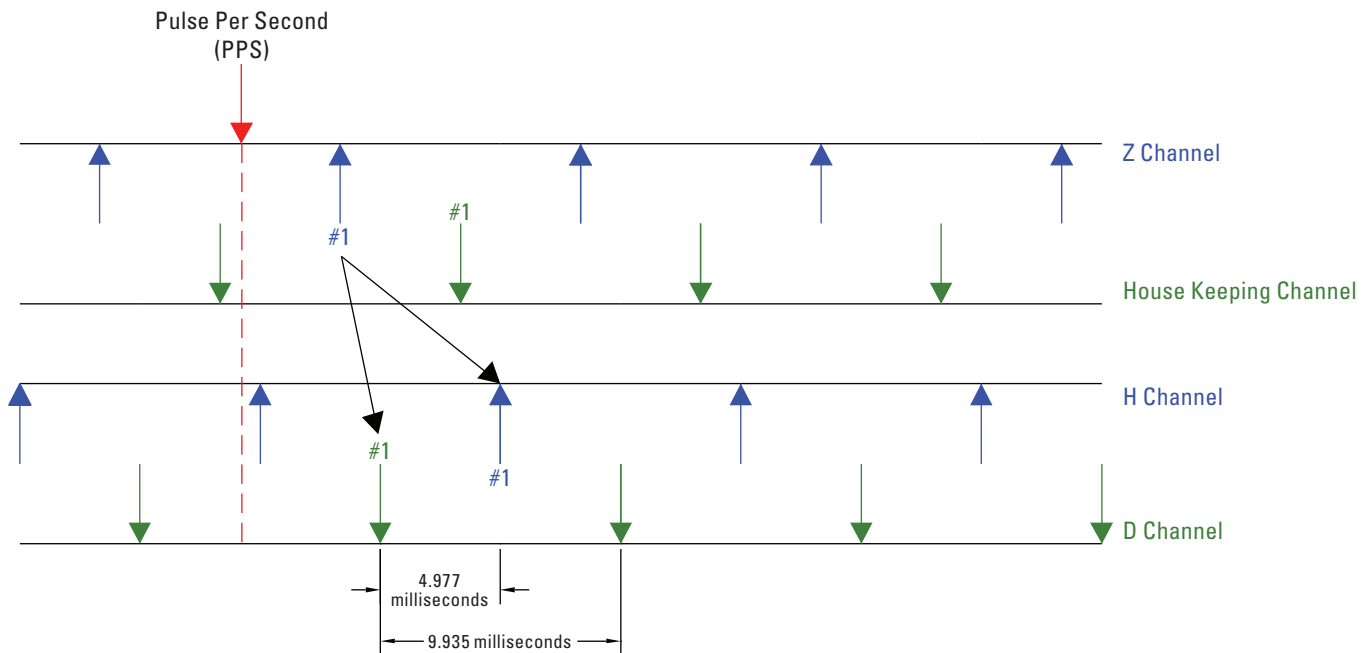


Figure 6. Examples of possible timing states for the Model 802 data-collection electronic module. [Z, vertical magnetic field component; H, north/south field component; D, east/west component; ms, milliseconds; PPS, pulse per second]

Table 1. Expected average delay and delay range for each magnetic component in the Model 802 electronic module.

[ms, millisecond; Z, vertical magnetic field component; H and D, horizontal north/south and east/west, respectively, magnetic field components]

Magnetic component	802 Data collection board	Minimum delay	Maximum delay	Average delay
Z	Master	0 ms	5 ms	2.5 ms
H	Slave	0 ms	15 ms	7.5 ms
D	Slave	0 ms	15 ms	7.5 ms

until a certain minimum threshold is met. High magnetic activity and high magnetic gradient incident on the sensor increase the decay rate. Either effect could cause the sampling period to be less than 965 ms. An observatory environment again is surveyed to ensure minimum magnetic gradients. Ideally, both the GSM-19 and Narod sensors are placed in environments with gradients in the vertical and horizontal directions less than 0.1 nT/m. This maximizes the sampling period of the GSM-19, effectively producing an average intensity value over the 965-ms sampling period. It is important to note that this average value lags behind the PPS by about 517.5 ms. Once a sample is collected, the GSM-19 uses the serial output of the T-bolt to time-stamp the one-second sample. The data then pass into an acquisition computer via a serial data connection.

Due to the complex nature of the sampling methodology used by the GSM-19, diagnostic timing tests are difficult to design. At the time of publication, no timing tests were conducted on the GSM-19, and this section appears for

informative purposes only. Testing will be designed and conducted in future efforts.

Data Transport and Digital Filtering

The data buffers for one second each of the Z, H, and D components are 100 samples in size. The serial data stream from the T-Bolt clock is used to time-stamp the top of all three data buffers. The data buffers then pass through an Ethernet connection into an acquisition computer where the data are processed by custom-developed data-collection software. First, new data arrays are created using 100 samples from the current second’s data and 99 samples from the previous second’s data. The new data arrays contain 199 data points. The arrays then pass into a digital Gaussian filter (see Glossary). The Gaussian filter has a sigma of 26.4557 seconds at the precision used in the USGSGP PCDCP systems and is centered on the PPS, that is, at the top of the second. The Gaussian filter is defined by a set of pre-calculated coefficients based on the array width and sigma value. The data are weighted by the coefficients and summed to produce digitally filtered one-second data values for all three components. One-second values are stored to memory and pass into three additional data arrays. Those data arrays then produce one-minute data.

Similar to the one-second data values, the one-minute data are produced by digitally filtering the 119-sample array, made up of 60 samples from the current minute and 59 samples from the previous minute. The one-minute Gaussian filter has a sigma of 15.8734 seconds, again at the PCDCP precision. As with the one-second data, the pre-calculated Gaussian coefficients are multiplied with the data arrays. Those weighted values then are summed to produce one-minute data values. The values are stored to memory.

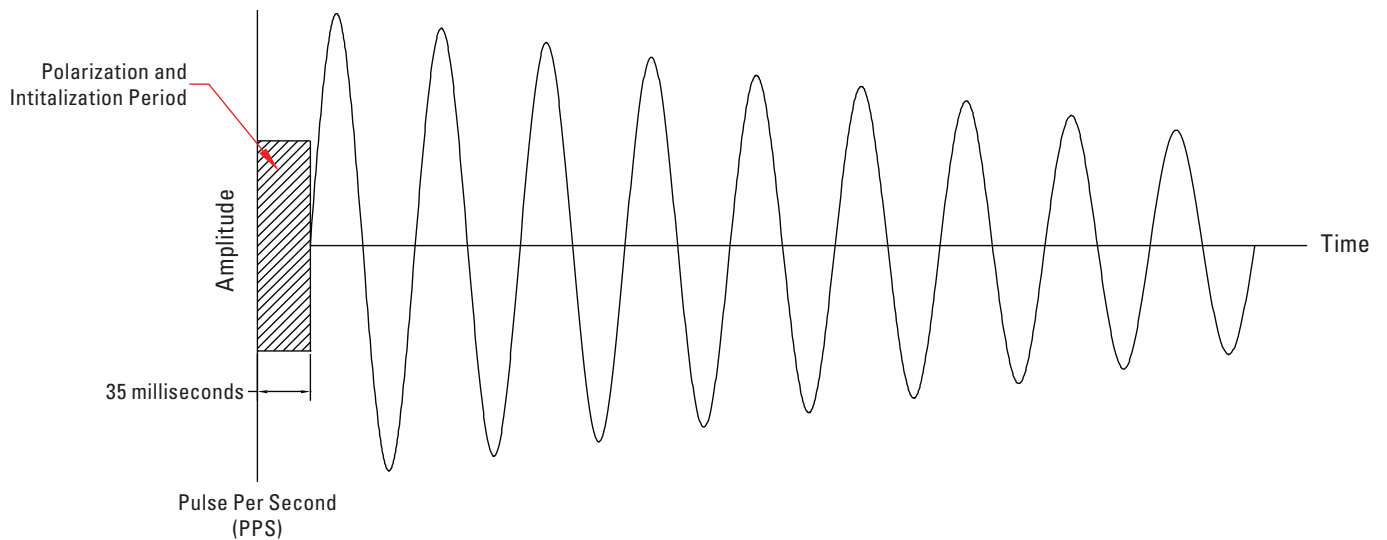


Figure 7. Gem Systems GSM-19 Overhauser magnetometer sampling methodology. [ms, milliseconds; PPS, pulse per second]

In addition to being stored into local memory, the one-minute and one-second data are transported via the internet to a central data repository, located at USGS/GP offices in Golden, Colorado. At the USGS/GP offices, the data are stored and published to the World Wide Web. Data are available at <http://geomag.usgs.gov>, accessed December 27, 2012.

Method for Testing Delay

Two known hardware sources produce delay within PCDCP. The first source is the delay introduced by the Narod magnetometer, specifically by the low-pass analog Butterworth filters within the Narod. Delay in the time domain is expected to be constant for frequencies of 0 Hz to the corner frequency of 50 Hz. The second known source of delay is from the 802 unit and is related to the continuous 100.1-Hz sampling. That delay varies but has a range of about 0–5 ms for the Z channel and about 0–15 ms for the H and D channels.

A series of tests measures the total delay introduced by PCDCP. The first set of tests measures delay from the Narod and 802 independently. A second test, designed by Jean Rasson (Rasson, 2009), is used to confirm results obtained by the USGS/GP-designed tests. A final test measures total delay introduced by all PCDCP components using the Rasson methodology but with USGS/GP test equipment.

Individual Component Tests

Sine-Wave Test

Introduction

A test isolates delay produced by the Narod magnetometer. The primary sources of delay within the Narod magnetometer are analog filters used on the analog output signal of the Narod. Filters include three-pole Butterworth low-pass filters (Butterworth). The Butterworth has a corner frequency of 50 Hz. For signals with frequencies from 0–50 Hz, the phase response of the Butterworth produces a nearly constant time lag. The expected delay introduced by the Narod is 12 ms.

Test Setup

A function generator is used to produce a sinusoidal wave and set to produce a single shot signal. The sine wave passes into a custom-made coil placed near the Narod sensor. (See table 2 for detailed specifications on the coil.) A resistor placed in series with the coil and an oscilloscope monitor the output signal from the coil. That resistor remains in place during testing. Signal from the function-generator output also is monitored using a second channel on the oscilloscope. Amplitude of the sine wave is 10 volts, and the frequency of the wave varies from 1 Hz to 50 Hz. As the sine wave passes through the coil, a magnetic signal is generated by the coil, and the

Table 2. Specifications of the Narod magnetometer customized test coil.

Physical characteristic	
Length of coil:	30.5 centimeters
Radius of coil:	10 centimeters
Number of turns:	28
Coil resistance:	1 ohm
Wire gauge:	14 gauge
Total circuit resistance (with leads):	7 ohms

Narod acquires the resultant sinusoidal signal. An oscilloscope monitors the analog output of the Narod on one channel and the signal from the function generator on a second channel and thereby measures the time difference between the function-generator signals and the Narod-measured sinusoidal waves.

Pre-Test Measurements

The oscilloscope measures delay added to the sinusoidal signal by the coil circuit. This is done by adding a 1-ohm test resistor to the return side of the coil circuit (fig. 8). The signal from the function generator is compared to the return signal across the resistor, and delay is measured. The coil circuit introduces 4.0 μ s of delay (as seen in figure 9).

Test Results

The delays measured with the oscilloscope at each test frequency for the H axis of the Narod sensor are presented in table 3. Delays typically are close to the expected value of 12 ms.

Square-Wave Test

Introduction

An additional test isolates the delay produced by the Narod magnetometer. The use of an impulse, similar to the square wave produced during this test, has been a common method used to characterize frequency response of analog filters. Application of the method to the Narod magnetometer was anticipated to yield interesting and unexpected results since the test setup produces a physical phenomenon to be detected rather than an electrical signal injected directly into the circuit. Test results between the sine-wave test and the square-wave test therefore are expected to show slight variation.

Test Setup

A Berkeley Nucleonics Corp. BNC 565 pulse/delay generator (BNC 565) produces a square pulse, and the PPS signal provides a time reference. The PPS signal passes into

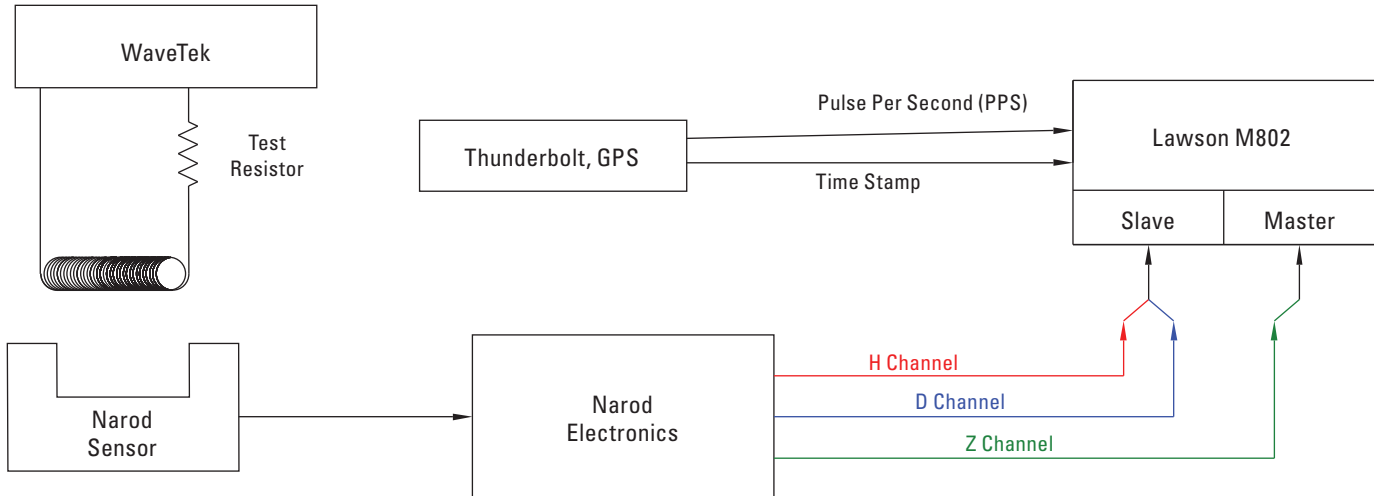


Figure 8. Sine-wave test setup for characterizing delay in the Narod magnetometer. [Z, vertical magnetic field component; H, north/south field component; D, east/west component]

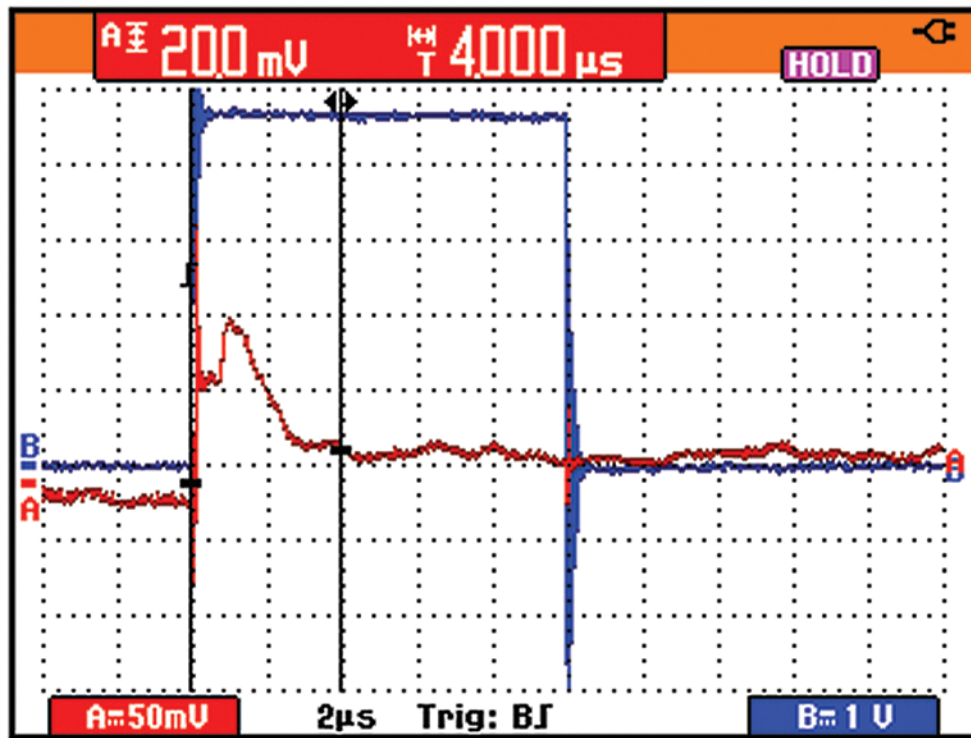


Figure 9. Signal delay in the Narod magnetometer as measured by oscilloscope across a 1-ohm test resistor on the trailing edge of the coil circuit. [A, amplitude; V, volt; mV, millivolt; T, time; μs , microsecond]

10 Discovery and Analysis of Time Delay Sources in the Data Collection Platform System

Table 3. Sine-wave results at test frequencies for the H (north/south) axis of the Narod magnetometer sensor.

[Hz, hertz; ms, milliseconds]

Sine wave frequency (Hz)	Phase lag (ms)
1	11
10	9.6
20	10
30	10.2
40	10.4
50	10.2

the oscilloscope as well as into the BNC 565, where it triggers a square pulse generated by the BNC 565. The square pulse in turn passes into the identical coil circuit as discussed in the previous section. The second channel of the oscilloscope monitors the analog output of the Narod magnetometer. The test measures the time delay between the PPS signal and the Narod signal for detection of the pulse.

Pre-Test Measurements

The oscilloscope measures the delay added to the pulse signal by the coil circuit, accomplished by adding a 1-ohm test resistor to the return side of a coil circuit. The PPS signal provides a time reference. Delay introduced by the BNC 565 is about $0.120 \mu\text{s}$, and the coil circuit introduces $4.0 \mu\text{s}$ of delay. The total delay introduced by the test setup is $4.12 \mu\text{s}$.

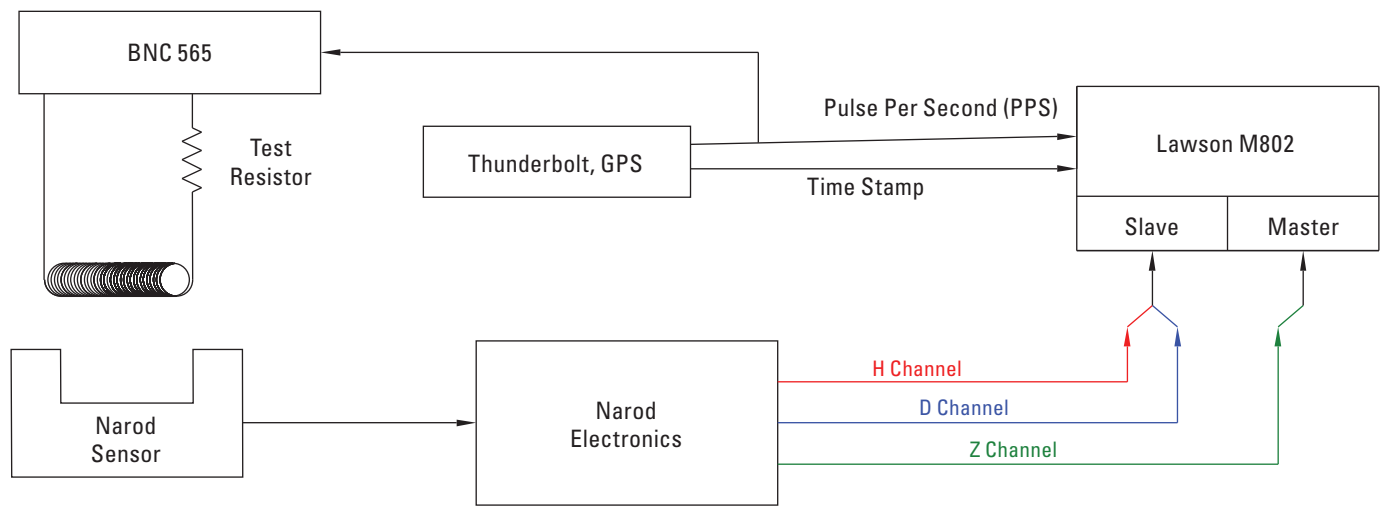


Figure 10. Square-wave test setup for characterization of delay in the Narod magnetometer using a Berkeley Nucleonics Corp. BNC 565 pulse/delay generator. [Z, vertical magnetic field component; H, north/south field component; D, east/west component; GPS, global positioning system]

Test Results

The delay measured with the oscilloscope for each of the three sensor axes and multiple sensors is presented in table 4. The delays are close to the expected value of 12 ms.

Lawson Model 802 Square-Wave Test

Introduction

This test is slightly different than the Narod magnetometer test described in the previous section. The goal of this test is to isolate the time lag introduced by the Lawson Model 802 electronic data-collection module. The 802 operates in a free-running mode. (Please refer to previous discussion of the triggering/time-stamping process for a full description.)

Table 4. Step response test results for square-wave testing of the Narod magnetometer.

[H, north/south magnetic field component; D, east/west field component; Z, vertical magnetic field component; ms, millisecond; Narod serial numbers relate to specific instruments]

Narod	H: full response	D: full response	Z: full response
Serial number			
2008-6	10.0 ms	10.8 ms	10.8 ms
2009-1	10.8 ms	11.2 ms	11.2 ms
2009-2	9.6 ms	8.4 ms	8.6 ms

When operating in free-running mode, measured time lags introduced by the 802 module are expected to vary cyclically between upper and lower bounds, while the average time lag is expected to be constant. The average time lag also is expected to be different for the H and D channels versus the Z channel. The expected time lags produced by the 802 are presented in table 1.

Test Setup

A Berkeley Nucleonics Corp. BNC 565 pulse/delay generator (BNC 565) again produces a square pulse in testing of the Model 802 module. The PPS signal from the T-Bolt clock provides an absolute time reference. The PPS signal passes into the oscilloscope and into the BNC 565, where the PPS signal triggers a square pulse generated by the BNC 565. The pulse is connected to all three analog inputs of the Lawson Model 802 unit. The 100-Hz samples capture the time moment of pulse incidence on each channel of the Lawson 802 unit.

Pre-Test Measurements

The BNC 565 has a programmatically adjustable time offset. That allows for placement of the square pulse generated by the BNC 565 at a known time offset from the PPS trigger. The total delay introduced by the BNC 565 was the 0.120- μ s delay measured in the square-wave test plus the adjustable time offset.

Test Results

The analysis used in this testing examines the three-times (3x) 100-sample data array produced each second by the Lawson 802 data-collection module. By varying the

programmatically adjustable time offset in the BNC 565 and observing that delay’s effect on detection of the square pulse in the Lawson 802 data arrays, the minimum, maximum, and average delays introduced by the 802 can be determined for each channel.

For testing of the H channel, an artificial time offset of 100 ms introduced to the BNC 565’s square pulse ensures that the signal has ample time to ramp up in the 802 and allow the PPS to be distinguished from the square pulse. The lower bound for the H channel is established by increasing the time offset on the BNC 565 until the square-pulse signal is first detected on one #10 sample within the 802’s H data array. The offset introduced by the BNC 565 was 104.2 ms. Subtracting the programmed 100-ms artificial time offset, the lower bound for the Lawson 802 H channel becomes 4.2 ms. The upper bound is found by decreasing the programmed time offset on the BNC 565 until all 15 seconds in the 15-second cycle fully detect the square-pulse signal on the #10 sample. The upper bound is 13.4 ms.

The results for the D channel match those obtained for the H channel. That result is as expected, as both the H and D channels are sampled by the same ADC and multiplexed on that ADC.

Results for the Z channel vary—as anticipated—from those obtained for the H and D channels. Lower and upper bounds were expected near zero and about 5 ms, respectively. The same procedure is followed as used for the H and D channels. Time offset is adjusted on the BNC 565 until the square pulse is first seen on one #10 sample within the 802’s Z data array. The lower bound for the Z channel was found to be -1 ms. That result means that the lower bound appeared before the PPS. Although that result is slightly unexpected, it is not unreasonable to find that the synchronization process within

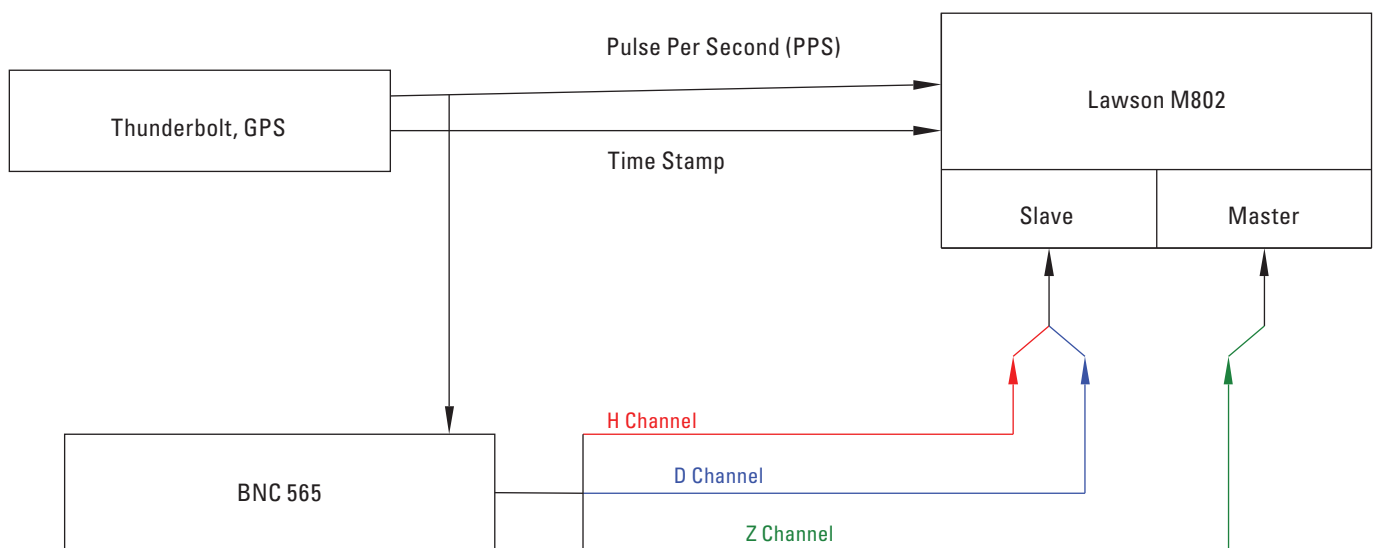


Figure 11. Square-wave test setup for characterization of delay in the Lawson Model 802 data-collection module using a Berkeley Nucleonics Corp. BNC 565 pulse/delay generator. [Z, vertical magnetic field component; H, north/south field component; D, east/west component; GPS, global positioning system]

the 802 could create that effect. The upper bound is found by decreasing the artificial time offset on the BNC 565 until all #10 samples within a 13-second cycle fully detect the square pulse. The upper bound appears at 8.7 ms, different than the expected 5 ms based upon information from the manufacturer (Lawson Labs, Inc., Malvern, Pa., oral commun., 2010).

Overall System Test

Two tests verify the total system delay. Unlike previous tests, these tests examine delay introduced by the entire system as that system would be arranged for characterizing the final data product. The two tests fundamentally are very similar. A square wave with a long period is generated. The period of that signal varies from 8 to 32 seconds, but two different function generators produce the signal for each test. The first function generator was designed by Jean R. Rasson (Rasson, 2009) and built by Canadian Natural Resources. Full documentation of the test was published by J.R. Rasson in Proceedings of the 2008 International Association of Geomagnetism and Aeronomy Instrumentation Workshop (Rasson, 2009). The Berkeley Nucleonics Corp. BNC 565 provides the second function generator. A data-fitting algorithm extracts the delay measurement from the one-second data file. The results are expected to agree with those obtained in the individual component tests.

Jean Rasson Test

Test Setup

The test is designed to be nonintrusive, such that access is needed only to the Narod sensor and to the collected data. A coil is placed near the Narod sensor. That coil is connected to a custom-designed “Black Box.” The Black Box has a GPS receiver and a current-generating circuit. The PPS signal from the GPS triggers a square wave. The period of the square wave is controllable and may be set to the following time series: 2, 4, 8, 16, ... seconds. Since the Black Box has an independent GPS, any systematic error in the T-Bolt clock could be identified. A Least-Squares data fit (see Glossary) applied to the data estimates the total-system delay. The data fit requires that the start time of the wave as well as the period of the square wave are known.

Pre-Test Measurements

An oscilloscope is used to measure differences between the PPS signal, which triggers the square wave, and the return of the square pulse from the coil circuit. In these measurements, the difference between the two signals was 4.0 μs . The oscilloscope measures the difference between the PPS from the Black Box and the PPS from the T-Bolt. The two signals typically shift slightly relative to each other but have a maximum difference of 108 ns. The two signals are shown in figure 12, where the blue signal is the T-Bolt PPS and the

red signal is the Black Box PPS. This signal plot reflects a systematic error between PCDCP and the Black Box.

Test Results

The test was run with 8-, 16-, and 32-second square-wave periods. The results for the 8- and 16-second periods seemed to agree with results obtained from individual tests. The results from the 16-second test varied slightly from the test results from the 8-second period, as well as from the individual component results. The results from the 32-second square wave varied significantly. These results put the Black Box of the Rasson test into question when used to generate waves of longer periods.

Berkeley Nucleonics Corp. BNC 565 Test

Introduction

The customized Black Box design was replicated easily utilizing the BNC 565 pulse/delay generator also used for the individual tests. The BNC 565 generated a wave initiated by a trigger. For completeness, the PPS from the T-Bolt and from the Black Box were used to trigger a square wave. The BNC 565 was set up to produce square waves with several different periods including 8, 10, and 12 seconds. The results were compared to those obtained from the individual tests and from the Jean Rasson overall system test.

Pre-Test Measurements

The pre-test measurements were completed during previous tests. The delay introduced by the BNC 565 was about 0.120 μs . The coil circuit introduced 4.0 μs of delay. The total delay introduced by the test setup therefore was 4.12 μs .

Test Results

The test was run for square-wave signals with periods of 8, 10, and 12 seconds. The same data-fitting algorithm was used as employed in the Jean Rasson test section. Data were processed, and the delay was established for each test. Results are presented in table 6.

Analysis and Summary of Results of Delay Testing

A summary of the test results appears in table 7. Since there is an expected and observed difference between the H and D components and the Z component caused by the Lawson 802 electronics, the results for Z are presented in parentheses in table 7.

A brief look shows that the results from system-level tests versus the superposition of individual tests indicate strong agreement. It also is important to realize that the overall

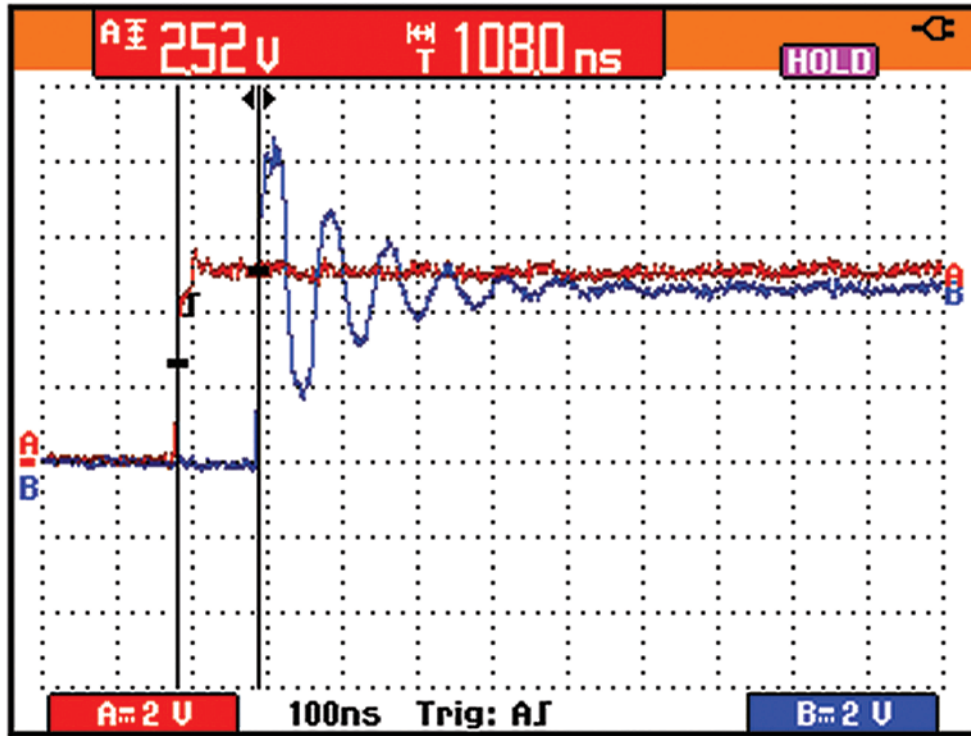


Figure 12. Customized Black Box pulse-per-second (PPS) signal (red) in relation to the T-Bolt clock PPS signal (blue), as shown on oscilloscope screen in the Rasson overall system test. [Abbreviations: v, volts; ns, nanoseconds]

Table 5. Jean Rasson test results for overall system delay.

[H, north/south magnetic field component; D, east/west field component; Z, vertical magnetic field component; ms, milliseconds]

Narod serial number (signal period)	H time lag (ms)	D time lag (ms)	Z time lag (ms)
2008-6			
(8 seconds)	18	18	10
(16 seconds)	18	18	10
(32 seconds)	7	7	-1
2009-2			
(8 seconds)	14	15	6
(16 seconds)	13	13	5
(32 seconds)	11	7	13
2009-1			
(8 seconds)	18	17	10
(16 seconds)	16	15	8
(32 seconds)	-2	2	-10

Table 6. Delay-test results using the Berkeley Nucleonics Corp. BNC 565 pulse generator.

[ms, millisecond; H, north/south magnetic field component; D, east/west field component; Z, vertical magnetic field component]

Narod serial number (signal period)	H time lag (ms)	D time lag (ms)	Z time lag (ms)
2008-6			
(10 seconds)	19	19	11
(12 seconds)	18	19	11
2009-2			
(8 seconds)	16	16	7
(10 seconds)	16	16	8
(12 seconds)	15	16	8
2009-1			
(8 seconds)	20	18	11
(10 seconds)	20	18	11
(12 seconds)	19	18	11

Table 7. Summary of all results from delay tests alone.

[ms, millisecond; --, not applicable; values in parentheses are for the Z component]

Method	Narod delay	Lawson 802 delay	Total system delay
Square-wave test	8.4–11.2 ms	--	--
Sine-wave test	8.6–11.0 ms	--	--
802 Square-wave test	--	4.6–14.6 ms (-0.1–8.7 ms)	--
Superposition on components	8.4–11.2 ms	4.6–14.6 ms (-0.1–8.7 ms)	13.0–25.8 ms (8.3–19.9 ms)
Jean Rasson test	--	--	13–18 ms (5–10 ms)
BNC 565 test	--	--	15–20 ms (7–11 ms)

system tests indicate average delays introduced by the system but do not provide upper and lower bounds for the measured delay. For that reason, individual component tests are essential as those tests do provide the range of measured delay. Both average delay and range of expected delay must be known to meet the proposed One-Second Intermagnet Standards for time stamping error (maximum 10-ms delay) from the PPS (C.W. Turbitt, Intermagnet, Geological Survey of Canada, Ottawa, Ontario, oral commun., 2012).

In the following paragraphs, we compare expected values with those obtained through testing and provide explanation, where possible, for discrepancies. We also summarize the effects of any systematic error associated with the test setup.

Narod Magnetometer

The delay introduced by the Narod magnetometer is expected to arise largely from the three-pole Butterworth low-pass filters within the Narod electronics. The Butterworth is expected to introduce a near-constant delay for all signals with frequencies within the pass band (that is, from 0 to 50 Hz). In practice, electrical components have varying tolerances depending upon component type. Resistors commonly exhibit tolerances at just ± 0.1 percent, but capacitor tolerances can be rated at ± 5 percent. Due to the potentially wide range of expected values for any capacitor, special attention is taken to match every capacitor network in the Butterworth filter with a specifically matched set of resistors. For this application, both capacitors and resistors are measured component by component to ensure that the Butterworth operates as expected. Although this step is taken very carefully, there are limitations related to selection of these components, and variations do exist between individual Butterworth filters. Note that with three filter networks per Narod, variation also is expected between channels for each Narod magnetometer.

The delays measured from Narod to Narod and between individual channels do vary as expected. Measured delays show a range of 8–11 ms for the tested Narods. The expected

delay from the Butterworth was 11 ms, on the high end of what actually was measured in the Sine-Wave Test and Square-Wave Test sections of this report.

A small difference appears between the results measured with the two waveform tests, likely due to differences in the response between the square pulse and the sine wave. Additionally, the oscilloscope in the testing had a 0.2-ms resolution, and the results agree within 0.2 ms. No systematic error should be introduced by the test setup beyond the 4.0 μ s introduced by the coil circuit. The same coil circuit was used for both the square-wave test and the sine-wave test; therefore, the delay introduced by the test setup should be the same for both tests, as confirmed by measurement.

Lawson Model 802 Data-Collection Electronic Module

Testing for delay in the Lawson Model 802 module involves differences from the method used for the Narod magnetometer, as only a single test measures delay introduced by the Lawson 802 module. The Lawson sampling and multiplexing methodology introduces an expected range of delay, not a constant delay like that of the Narod. Therefore, test design measures the upper and lower bounds of the range of delay. The delay introduced on the vertical component (Z) also is expected to vary from that introduced on the north/south (H) and east/west (D) components. Design of such a test is more complicated than the simpler, more common tests used for the Narod instrument.

The measurement shows that Z has a lower bound of -0.1 ms. In this case, negative value represents a data point which is labeled number 1 and collected 0.1 ms before the PPS arrival. This unexpected but not unrealistic result arises from the PPS synchronization operation within the master analog-digital converter (ADC) of the 802. The upper bound measures 8.7 ms, and again, the measured value varies from the expected 5 ms upper bound. The average delay introduced by the 802 on the Z channel is 4.3 ms.

Sample labeling for the H and D channels is “triggered” by the Z channel. That means an H and D sample could not be labeled as number 1 until the number 1 sample has been collected by Z. The lower bound for both the H and D channels measures as 4.58 ms. The upper bound for the H and D channels, however, measures 14.55 ms. These values vary slightly from expected values of 5–15 ms, and likely are due to the difference between the expected and measured values for the Z channel.

Overall System Tests

The overall system tests use a data-fitting algorithm known as Least-Squares Data Fit (see Glossary) to fit an average delay. As noted previously, such tests do not provide upper and lower bounds for measured delay and therefore cannot be used independently of the component-level test to measure

the delay for the PCDCP system. For example, if the acquisition system has a delay range of -20 ms to +20 ms of PPS, the average could be 0 ms. However, a sizeable portion of the samples would not be taken within 10 ms of PPS and therefore would not adhere to the proposed Intermagnet Standards.

The average delays measured using the two overall system tests agree quite well (see table 7), although differences do exist. Both the Jean Rasson test and the BNC 565 test produce average delay measurements of about 18 ms for the H and D components and 10 ms for the Z component. The overall system tests produce poor and inconsistent results for signals with periods greater than 16 seconds. Further exploration and testing are required to identify the problem properly, but we suspect the sampling methodology of the 802 module is the source of the discrepancy.

The only expected source of systematic error relates to existence of two different PPS sources for these tests. Measurements therefore were made to establish the difference between the T-Bolt PPS and the Black Box PPS. The PPS signals drift relative to one another; maximum observed differences, however, between T-Bolts were 10 μ s. Although this delay is an order of magnitude below the level at which the measurements were made, it does point out the need for tests to be conducted on PPS sources prior to system testing, to verify their absolute accuracy. Otherwise, inherent PPS errors create systematic errors which cannot be identified during testing and thereby create inaccuracies in measurements.

Summary

In theory, the two Overall System Tests were the same. Some possibilities for variation exist, particularly when one looks at the PPS source and its absolute accuracy and stability. The component-level tests were different, however, and leave less room for error. There was no dependence on an absolute time source with the component-level tests; therefore, any PPS inaccuracies do not impact the results of the tests. It was true that digital filtering and processing could introduce time delays which would not be detected by component-level testing. Both types of tests, however, were required to properly and accurately measure delay introduced by the acquisition system.

References Cited

Gem Systems Advanced Magnetometers, Inc., 2011, GSM-19 Overhauser Magnetometer product sheet, available at www.gemsys.ca/products/rugged-overhauser-magnetometer/, last accessed December 21, 2012.

Narod, B., 2000, Narod triaxial ring core magnetometer—Product manual/design document: Vancouver, Narod Geophysics Ltd., pagination unavailable.

Rasson, J.L., 2009, Testing the time-stamp accuracy of a digital variometer and its data logger, *in* Love, J.J., ed., Workshop on Geomagnetic Observatory Instruments—Data Acquisition, and Processing, Golden, Colo., XIIIth, Proceedings: International Association of Geomagnetism and Aeronomy [IAGA], published as U.S. Geological Survey Open-File Report 2009–1226, p. 225–231. Also available online at <http://pubs.er.usgs.gov/publication/ofr20091226/>.

Trimble Navigation Limited, 2011, Thunderbolt E GPS Disciplined Clock: Sunnyvale, Calif., Trimble Navigation Limited, available at www.trimble.com/timing/thunderbolt-e.aspx, last accessed December 21, 2012, unpaginated.

Glossary

Charge pumpout an effect produced by multiplexing between two channels. In the case of PCDCP, channel A and channel B can have a maximum difference of 10 VDC, (that is, -5 VDC to +5 VDC, for example). Ignoring the first four samples after the multiplexer transition allows the ADC adequate time to make the transition from -5 VDC to +5 VDC to produce stable voltage readouts.

Gaussian filter a digital filter applied to the data in a post-processing procedure. The filter has two design constraints; the first is number of samples to which the filter is being applied. For USGSGP one-second data, 199 samples at 100.1 Hz are used, and therefore the width of the filter is 199. The second design constraint, sigma (σ), controls the weighting distribution of the filter. A sigma value of 26.4557 seconds is selected. See Appendix A for more details on the computations and design of this filter.

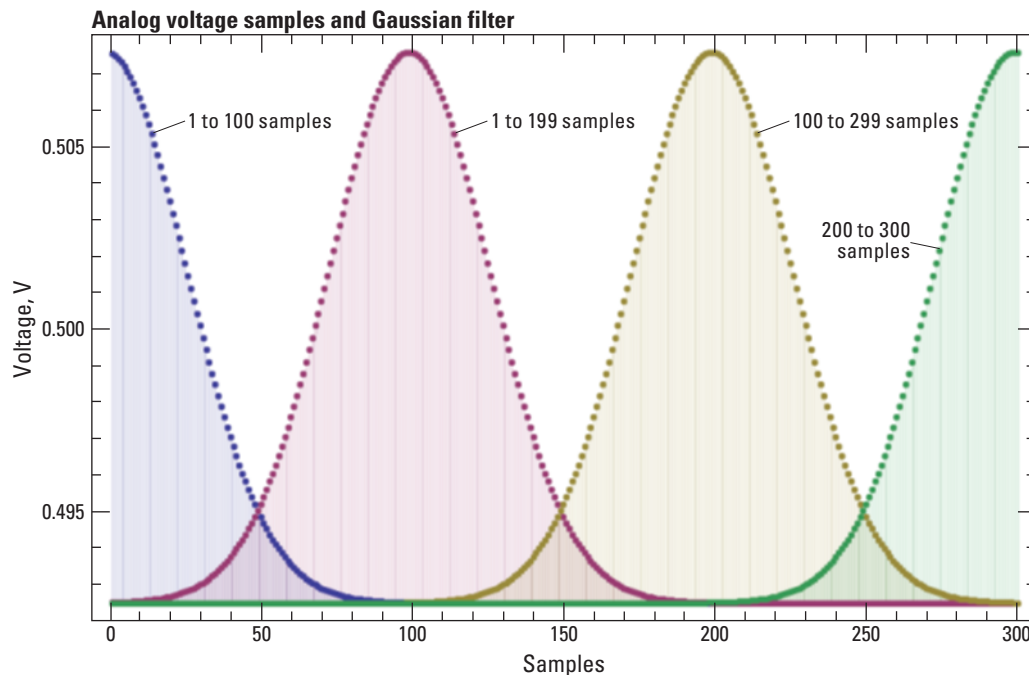


Figure 13. Example of Gaussian filter weighting function applied over four seconds of 100-Hz data.

Least-squares data fit a standard method used to statistically fit, or solve for, unknown variables when many data points are available. The method finds a best fit by minimizing the sum of squared residuals.

Multiplexing an electrical process equivalent to physically switching between two or more channels. There are two different multiplexers in the 802 electronic unit. Both the master and the slave units each have a two-channel multiplexer. These multiplexers switch between two channels every 5 ms. The master has an additional multiplexer attached to one of its channels which switches between five channels every 5 ms.

Appendix A. Design of Personal Computer Data-Collection Platform Gaussian Filters

Gaussian Filters

The USGSGP applies digital filters to the raw samples collected by the Personal Computer Data-Collection Platform (PCDCP) system to produce its one-minute and one-second data products. The digital filters are a set of precalculated numerical coefficients which are applied to the raw samples collected by PCDCP. These coefficients form the weighting functions applied to the raw data, which place higher importance on raw data points respectively collected near the top of the minute or top of the second. The computation of these coefficients is described below for the one-minute and one-second data, respectively.

Appendix A–1. Design of the Personal Computer Data-Collection Platform One-Minute Gaussian Filter

The one-minute geomagnetic data produced by the PCDCP acquisition system are obtained by passing one-second data samples through a digital Gaussian anti-aliasing filter. The filter is based on discrete-time samples of the Gaussian Fourier transform pair:

$$F(\omega) = e^{-\frac{1}{2}(\sigma\omega)^2} \quad \text{A.1}$$

$$F(t) = \frac{1}{\sigma\sqrt{2\pi}} e^{-\frac{1}{2}\left(\frac{t}{\sigma}\right)^2} \quad \text{A.2}$$

where ω represents an angular (radial) frequency, and where $\omega = 2\pi f$ (f = frequency). The value of σ is determined by the parameters of the corner frequency selected for the filter and represents the full width at the half-maximum point of the Gaussian curve.

The corner frequency of the filter is defined as the point where the filter's output amplitude is reduced by 3 decibels with respect to the input.

The decibel (*dB*) formula for amplitude is:

$$db = 20 \text{Log}_{10} \left(\frac{A_{out}}{A_{in}} \right)$$

From this, $db = -3$ when:

amplitude, $\frac{A_{out}}{A_{in}} = 0.707946$ at the defined precision used in similar USGSGP calculation.

To provide anti-aliasing, the frequency at the corner is set equal to the Nyquist frequency of the filter's output. The

Nyquist frequency equals one-half of the output frequency, so a filter producing output samples with a period of 1 minute (frequency = 1/60 Hz), has a Nyquist frequency of 1/120 Hz.

Step Two: Calculate the Value of σ , Sigma

Inserting the corner-frequency parameters into Equation A.1 gives:

$$F(\omega) = 0.707946 \text{ when } \omega = 2\pi f = \frac{2\pi}{120}$$

$$\text{or, } 0.707946 = e^{-\frac{1}{2}\left(\sigma \frac{2\pi}{120}\right)^2}.$$

Solving for σ , $\sigma = 15.8734$ seconds.

Step Three: Calculate and Normalize Filter Coefficients

The filter coefficients are obtained by inserting the value obtained for σ into Equation A.2:

$$f(t) = e^{-\frac{1}{2}\left(\frac{t}{15.8734}\right)^2}$$

Note: the constant multiplier $1/(2\pi\sigma)$ in Equation A.2 is ignored because a normalization will be applied to each coefficient as the final step of calculation.

Now, the function is evaluated for discrete values of t , using the sample rate of the filter's input and assigning $t = 0$ as the center of the filter:

$$t = 0$$

$$t = \pm 1 \text{ second,}$$

$$t = \pm 2 \text{ seconds, and so on.}$$

Table A-1 shows values for $F(t)$ evaluated to ± 45 seconds from the center of the filter. The evaluation stops at 45 seconds because the decreasing magnitude of $F(t)$ makes contributions from samples beyond 45 seconds effectively negligible with respect to samples near the center of the filter.

The normalized coefficients are the $F(t)$ values of Equation A.3, scaled so that the sum of the 91 coefficients (that is, -45 to $+45$ seconds) equals 1. Each value of $F(t)$ is divided by K , where:

$$K = \sum_{t=-45}^{t=45} F(t) = 39.6238$$

Normalized filter coefficients are listed in the table, and a data plot also is shown in figure A–1.

20 Discovery and Analysis of Time Delay Sources in the Data Collection Platform System

Table A-1. Filter coefficients for the Personal Computer Data-Collection Platform one-minute Gaussian filter. Precision is set to six significant figures, consistent with similar USGSGP calculations.

[±, plus or minus; see equation A.3 for function $F(t)$]

Time (seconds)	$F(t)$ (equation A.3)	Normalized coefficient	Time (seconds)	$F(t)$ (equation A.3)	Normalized coefficient
0	1.000	0.025	± 12	0.751	0.019
± 1	0.998	0.025	± 13	0.715	0.018
± 2	0.992	0.025	± 14	0.678	0.017
± 3	0.982	0.025	± 15	0.640	0.016
± 4	0.969	0.024	± 16	0.602	0.015
± 5	0.952	0.024	± 17	0.564	0.014
± 6	0.931	0.023	± 18	0.526	0.013
± 7	0.907	0.023	± 19	0.489	0.012
± 8	0.881	0.022	± 20	0.452	0.011
± 9	0.852	0.021	± 21	0.417	0.011
± 10	0.820	0.021	± 22	0.383	0.010
± 11	0.787	0.020			

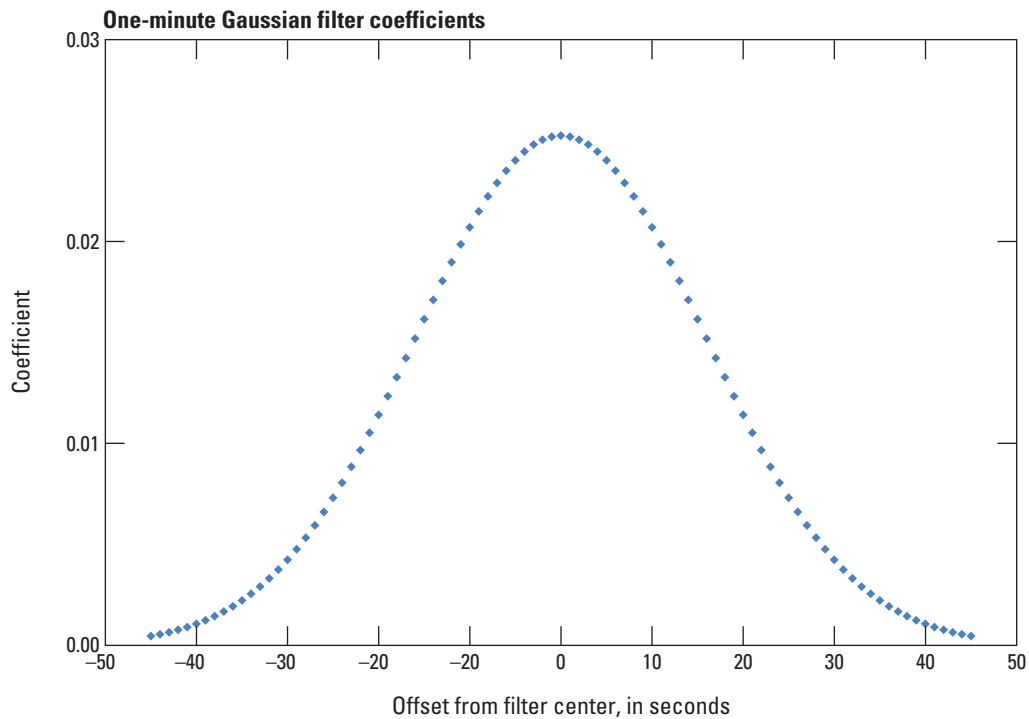


Figure A-1. Normalized coefficients of the one-minute Gaussian filter.

Appendix A-2. Design of the Personal Computer Data-Collection Platform One-Second Gaussian Filter

The one-second geomagnetic data produced by the Personal Computer Data-Collection Platform (PCDCP) acquisition system are obtained by passing 0.01 second (100 Hz) data samples through a digital Gaussian anti-aliasing filter. It is not necessary to repeat the similar development shown previously for the one-minute filter. The value of σ for the one-second filter is obtained simply by scaling the one-minute σ by a factor of 60:

$$\sigma_{1\text{-second}} = \frac{1}{60} \sigma_{1\text{-minute}} = 0.264557$$

and evaluating the expression:

$$f(t) = e^{-\frac{1}{2} \left(\frac{t}{0.264557} \right)^2}$$

For time values:

$$t = 0,$$

$$t = \pm 0.01 \text{ second},$$

$$t = \pm 0.02 \text{ seconds, and so on.}$$

Figure A-2 and table A-2 show the values of $F(t)$, normalized coefficients, and the plot of coefficients for the one-second filter. The coefficients are evaluated to ± 0.99 seconds from the center of the filter.

In this case, the value of the normalizing factor K is:

$$K = \sum_{t=-0.99}^{t=0.99} F(t) = 66.3033$$

From the coefficient magnitudes it is clear that samples outside about ± 0.75 seconds have a near-negligible contribution to the filter output.

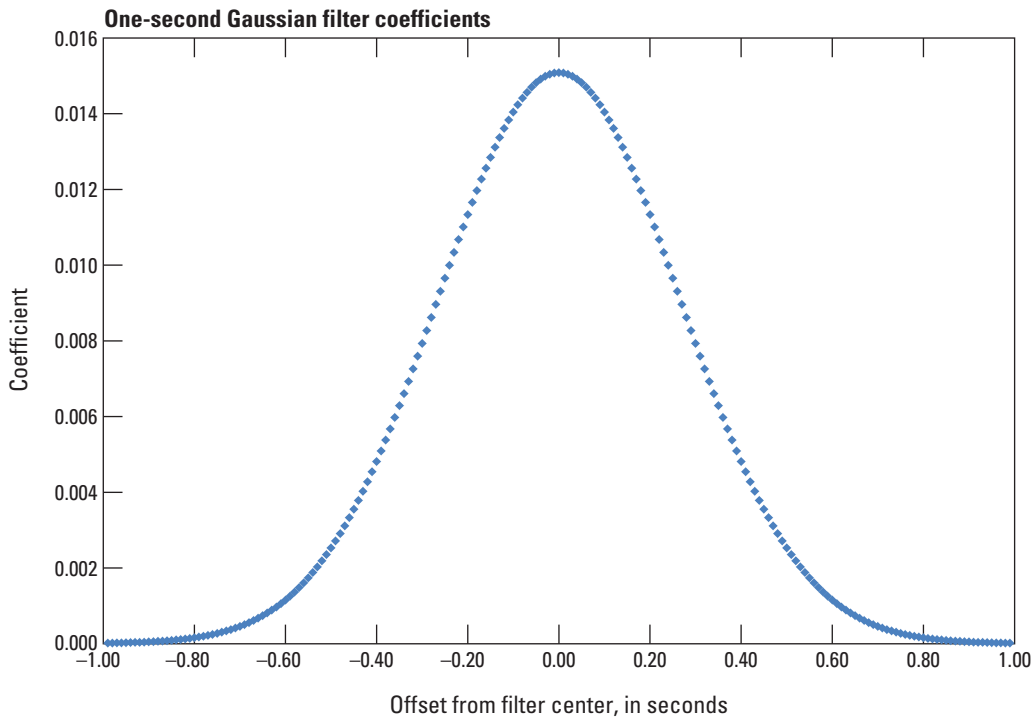


Figure A-2. Normalized coefficients of the one-second Gaussian filter.

22 Discovery and Analysis of Time Delay Sources in the Data Collection Platform System

Table A-2. Filter coefficients for the Personal Computer Data-Collection Platform one-second Gaussian filter.

Precision is set to six significant figures, consistent with similar USGSGP calculations. [\pm , plus or minus; see equation A.3 for function $F(t)$]

Time (seconds)	$F(t)$	Normalized coefficients	Time (seconds)	$F(t)$	Normalized coefficients
-0.99	0.001	0.000	-0.58	0.090	0.001
-0.98	0.001	0.000	-0.57	0.098	0.001
-0.97	0.001	0.000	-0.56	0.106	0.002
-0.96	0.001	0.000	-0.55	0.115	0.002
-0.95	0.002	0.000	-0.54	0.125	0.002
-0.94	0.002	0.000	-0.53	0.134	0.002
-0.93	0.002	0.000	-0.52	0.145	0.002
-0.92	0.002	0.000	-0.51	0.156	0.002
-0.91	0.003	0.000	-0.50	0.168	0.003
-0.90	0.003	0.000	-0.49	0.180	0.003
-0.89	0.003	0.000	-0.48	0.193	0.003
-0.88	0.004	0.000	-0.47	0.206	0.003
-0.87	0.004	0.000	-0.46	0.221	0.003
-0.86	0.005	0.000	-0.45	0.235	0.004
-0.85	0.006	0.000	-0.44	0.251	0.004
-0.84	0.006	0.000	-0.43	0.267	0.004
-0.83	0.007	0.000	-0.42	0.284	0.004
-0.82	0.008	0.000	-0.41	0.301	0.005
-0.81	0.009	0.000	-0.40	0.319	0.005
-0.80	0.010	0.000	-0.39	0.337	0.005
-0.79	0.012	0.000	-0.38	0.356	0.005
-0.78	0.013	0.000	-0.37	0.376	0.006
-0.77	0.014	0.000	-0.36	0.396	0.006
-0.76	0.016	0.000	-0.35	0.417	0.006
-0.75	0.018	0.000	-0.34	0.438	0.007
-0.74	0.020	0.000	-0.33	0.459	0.007
-0.73	0.022	0.000	-0.32	0.481	0.007
-0.72	0.025	0.000	-0.31	0.503	0.008
-0.71	0.027	0.000	-0.30	0.526	0.008
-0.70	0.030	0.000	-0.29	0.548	0.008
-0.69	0.033	0.001	-0.28	0.571	0.009
-0.68	0.037	0.001	-0.27	0.594	0.009
-0.67	0.040	0.001	-0.26	0.617	0.009
-0.66	0.045	0.001	-0.25	0.640	0.010
-0.65	0.049	0.001	-0.24	0.663	0.010
-0.64	0.054	0.001	-0.23	0.685	0.010
-0.63	0.059	0.001	-0.22	0.708	0.011
-0.62	0.064	0.001	-0.21	0.730	0.011
-0.61	0.070	0.001	-0.20	0.751	0.011
-0.60	0.076	0.001	-0.19	0.773	0.012
-0.59	0.083	0.001	-0.18	0.793	0.012

Table A–2. Filter coefficients for the Personal Computer Data-Collection Platform one-second Gaussian filter.—ContinuedPrecision is set to six significant figures, consistent with similar USGSGP calculations. [\pm , plus or minus; see equation A.3 for function $F(t)$]

Time (seconds)	$F(t)$	Normalized coefficients	Time (seconds)	$F(t)$	Normalized coefficients
-0.17	0.813	0.012	0.24	0.663	0.010
-0.16	0.833	0.013	0.25	0.640	0.010
-0.15	0.852	0.013	0.26	0.617	0.009
-0.14	0.869	0.013	0.27	0.594	0.009
-0.13	0.886	0.013	0.28	0.571	0.009
-0.12	0.902	0.014	0.29	0.548	0.008
-0.11	0.917	0.014	0.30	0.526	0.008
-0.10	0.931	0.014	0.31	0.503	0.008
-0.09	0.944	0.014	0.32	0.481	0.007
-0.08	0.955	0.014	0.33	0.459	0.007
-0.07	0.966	0.015	0.34	0.438	0.007
-0.06	0.975	0.015	0.35	0.417	0.006
-0.05	0.982	0.015	0.36	0.396	0.006
-0.04	0.989	0.015	0.37	0.376	0.006
-0.03	0.994	0.015	0.38	0.356	0.005
-0.02	0.997	0.015	0.39	0.337	0.005
-0.01	0.999	0.015	0.40	0.319	0.005
0.00	1.000	0.015	0.41	0.301	0.005
0.01	0.999	0.015	0.42	0.284	0.004
0.02	0.997	0.015	0.43	0.267	0.004
0.03	0.994	0.015	0.44	0.251	0.004
0.04	0.989	0.015	0.45	0.235	0.004
0.05	0.982	0.015	0.46	0.221	0.003
0.06	0.975	0.015	0.47	0.206	0.003
0.07	0.966	0.015	0.48	0.193	0.003
0.08	0.955	0.014	0.49	0.180	0.003
0.09	0.944	0.014	0.50	0.168	0.003
0.10	0.931	0.014	0.51	0.156	0.002
0.11	0.917	0.014	0.52	0.145	0.002
0.12	0.902	0.014	0.53	0.134	0.002
0.13	0.886	0.013	0.54	0.125	0.002
0.14	0.869	0.013	0.55	0.115	0.002
0.15	0.852	0.013	0.56	0.106	0.002
0.16	0.833	0.013	0.57	0.098	0.001
0.17	0.813	0.012	0.58	0.090	0.001
0.18	0.793	0.012	0.59	0.083	0.001
0.19	0.773	0.012	0.60	0.076	0.001
0.20	0.751	0.011	0.61	0.070	0.001
0.21	0.730	0.011	0.62	0.064	0.001
0.22	0.708	0.011	0.63	0.059	0.001
0.23	0.685	0.010	0.64	0.054	0.001

24 Discovery and Analysis of Time Delay Sources in the Data Collection Platform System

Table A-2. Filter coefficients for the Personal Computer Data-Collection Platform one-second Gaussian filter.—Continued

Precision is set to six significant figures, consistent with similar USGSGP calculations. [\pm , plus or minus; see equation A.3 for function $F(t)$]

Time (seconds)	$F(t)$	Normalized coefficients
0.65	0.049	0.001
0.66	0.045	0.001
0.67	0.040	0.001
0.68	0.037	0.001
0.69	0.033	0.001
0.70	0.030	0.000
0.71	0.027	0.000
0.72	0.025	0.000
0.73	0.022	0.000
0.74	0.020	0.000
0.75	0.018	0.000
0.76	0.016	0.000
0.77	0.014	0.000
0.78	0.013	0.000
0.79	0.012	0.000
0.80	0.010	0.000
0.81	0.009	0.000
0.82	0.008	0.000
0.83	0.007	0.000
0.84	0.006	0.000
0.85	0.006	0.000
0.86	0.005	0.000
0.87	0.004	0.000
0.88	0.004	0.000
0.89	0.003	0.000
0.90	0.003	0.000
0.91	0.003	0.000
0.92	0.002	0.000
0.93	0.002	0.000
0.94	0.002	0.000
0.95	0.002	0.000
0.96	0.001	0.000
0.97	0.001	0.000
0.98	0.001	0.000
0.99	0.001	0.000

Publishing support provided by:
Denver Publishing Service Center

For more information concerning this publication, contact:
Center Director, USGS Geologic Hazards Science Center
Box 25046, Mail Stop 966
Denver, CO 80225
(303) 273-8579

Or visit Geologic Hazards Science Center Web site at:
<http://geohazards.cr.usgs.gov/>

